Electronic Supplementary Material (ESI) for ChemComm.

Surface Plasmons & Visible Light For Polymer Functionalization of Mespores and Manipulation of Ionic Permselectivity

Nicole Herzog[a], Jonas Kind[a], Christian Hess[b], Annette Andrieu-Brunsen1[a]

[a]Technische Universität Darmstadt, Ernst-Berl-Institute, Alarich-Weiss-Str. 4, D-64287 Darmstadt, Germany

[b]Technische Universität Darmstadt, Eduard Zintl Institute for Inorganic and Physical Chemistry, Alarich-Weiss-Str. 8, D-64287 Darmstadt, Germany

Corresponding author: brunsen@cellulose.tu-darmstadt.de

Cyclic voltammetry of unmodified mesoporous silica

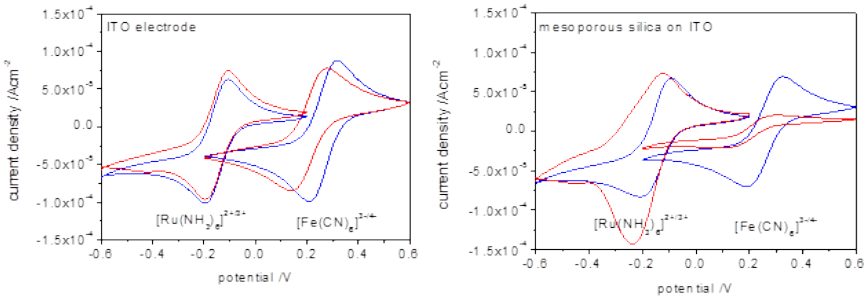

Figure S1: Cyclic voltammetry measurements at a scanrate of 25 mV/s and a pH < 3 (blue) and pH 8-9 (red) of an untreated ITO electrode (left) and an unmodified mesoporous silica film (right) deposited on an ITO electrode as comparison to Figure 5.

Polymer Characterization

Table S1: Gel permeation chromatography results for the solution polymer of non-plasma treated samples and co-initiator binding of 225 minutes polymerizing DMAEMA.

dye	$\bar{M}n$	$\bar{M}w$	PDI
2-chlorothioxanthone	2,5193 * 10^5	6,8306 * 10^5	2,7
4‘,5‘-dibromfluoresceine	2,8635 * 10^5	7,6562 * 10^5	2,7

Table S2: Gel permeation chromatography results for the solution polymer of non-plasma treated and plasma-treated samples after co-initiator binding for 45 minutes at 80°C polymerizing DMAEMA. It has to be mentioned that the polymer was not very well soluble indicating crosslinking during this uncontrolled polymerization process. GPC was measured using DMF/LiCl (3g/L) and the GRAM 1000 A VS with a GRAM 1000 A HS column (PSS, Mainz Germany) with a 1200 Agilent RID detector. Calibration was performed using PMMA standards (PSS).

Substrate & Dye	Mn in g/mol	Mw in g/mol	PDI	Monomers /chain mass spectroscopy after degrafting
planar silicon wafer 4',5'-dibromfluoresceine	$3{,}0419*10^4$	$4{,}0641*10^4$	1,3	-
mesoporous silica 4',5'-dibromfluoresceine	$7{,}5447*10^4$	$4{,}3123*10^5$	5,7	-
mesoporous silica – plasma – 4',5'-dibromfluoresceine	$7{,}2732*10^4$	$4{,}1228*10^5$	5,7	-
planar silicon wafer 2-chlorothioxanthone	$2{,}8248*10^4$	$7{,}9502*10^4$	2,8	-
mesoporous silica 2-chlorothioxanthone	$3{,}8526*10^4$	$1{,}2713*10^5$	3,3	-
mesoporous silica – plasma – 2-chlorothioxanthone	$3{,}4712*10^4$	$8{,}2979*10^4$	2,4	-
mesoporous silica methylene blue	$3{,}4293*10^5$	$1{,}0859*10^6$	3,2	5

A DMAEMA monomer has a molar weight of 157,2 g/mol. Assuming a C-C bond length of 0,154 nm, a molecular weight of 30.000 g/mol would correspond to approximately 190 monomers per chain. This would correspond to a chain length of ~ 59 nm in a fully extended state. The thickness increase upon polymerization between 4-10 nm was detected by ellipsometry. This is much lower as 59 nm, thus, indicating either a non stretched polymer state (no brush regime) and / or shorter polymer chains. Due to the spatial confinement shorter polymer chains are very likely. This is confirmed by an exemplary degrafting experiments for mesoporous silica films modified with PDMAEMA and polymerization initiation with methylene blue. For the degrafting we followed a procedure based on

TBAF as adapted from the literature.[1] The total degrafted substrate area was 650 cm². Precipitation of degrafted polymers revealed very low amount of polymer. Subsequent analysis by mass spectroscopy revealed molecular weights between 760-875 g/mol corresponding to ~5 monomers per chain (Table S3b). This low molecular weight was supported by GPC measurements showing a shoulder in the eluent peak.

Ellipsometry results

Polymerization inside the mesopores was additionally verified by ellipsometry measurements. The measured values for Δ and ψ could be reproduced with a one layer model giving the film thickness and the refractive index. The film thickness was determined to be around 260 nm after polymerization and the refractive index increased upon each modification step from 1.26 to 1.36 after co-initiator modification and exceeding 1.40 up to 1.46 after polymerization. Evaluating the refractive index change at different positions on a several cm² substrate area variations in refractive index are observed indicating the potential of improving polymer homogeneity. Nevertheless, for all positions an increase in refractive index is observed. Based on the effective medium approximation[2] a total pore filling of 30-45% in case of METAC polymerization initiated with methylene blue is detected assuming a refractive index for the filling components of 1.414. This might be an underestimation for the co-initiator refractive index. Nevertheless, this proves that the pore volume is not entirely filled after modification and thus molecular diffusion should still be possible. The exact values are summarized in Table S3.

Table S3: Ellipsometry results before and after co-initiator modification and after polymerization.

Sample	Layer Thickness /nm	Error Layer Thickness	Refractive Index	Error Refractive Index	RMSE
mesoporous silica	257,9	0,7	1,261	0,001	0,669

Sample	Layer Thickness /nm	Error Layer Thickness	Refractive Index	Error Refractive Index	RMSE	Sample
with coinitiator	1	250,3	0,6	1,376	0,002	0,334
	2	250,8	0,5	1,369	0,002	0,269
	3	251	0,5	1,378	0,002	0,236
average		250,7	0,5	1,37	0,002	
standard deviation		0,4		0,005		

Sample	Layer Thickness /nm	Error Layer Thickness	Refractive Index	Error Refractive Index	RMSE	Sample
with polymer	1	255,8	1,2	1,413	0,004	0,463
	2	258,6	0,6	1,391	0,001	0,242
	3	258	0,4	1,468	0,001	0,139
average		257,5	0,7	1,424	0,002	
standard deviation		1,5		0,04		

Data modeling for refractive index and film thickness determination was performed by using a one layer model which indicates a relatively homogeneous functionalization along the film thickness.

Ellipsometry measurements: Film thickness and refractive index was determined on silicon wafer substrates and measured using a Nanofilm EP3 imaging ellipsometer. One zone angle of incidence (AOI) variation measurements were captured between AOIs of 40 and 80° with a 658 nm laser. The apparent film thickness and refractive indices were calculated from the measured angles Ψ and Δ using the EP4 analysis software supplied with the instrument. The fitting parameters for the silicon oxide layer thickness on the wafer substrate (d(SiOx) = 2.8

nm) were measured separately. The measured data was fitted with a one-layer box model. The fitting program was allowed to vary film thickness of the mesoporous silica thin films between 100-500 nm and the refractive index between 1.1-1.7. All films were measured at three identical marked positions after each modification step. Changes were calculated for each specific position. To determine the porosity out of refractive indices the Brüggemann effective medium approximation was used as discussed elsewhere.[3-4] Measurements were performed at a temperature of 24 °C and a humidity of 32 %.

XPS results

Table S4: Atomic ratios as obtained by XPS analysis corresponding to Figure 3.

Sample	**C 1s** 285 eV at%	**O 1s** 533 eV at%	**N 1s** 400 eV at%	**Na 1s** 1073 eV at%	**Cl 2p** 200 eV at%	**Si 2p** 103 eV at%
#1: Reference	10.0	60.2	-	3.0	0.7	26.0
#2: Ini – 45 min	24.9	52.0	1.7	-	-	21.4
#3: Ini – 225 min	24.5	50.6	2.2	1.4	-	21.4

XPS analysis reveals peaks at around 103 eV, 154 eV, 200 eV, 285 eV, 400 eV, 533 eV, and 1073 eV, which are attributed to Si2p, Si2s, Cl2p, C1s, N1s, O1s, and Na1s photoemissions, respectively.[Handbook of X-ray Photoelectron Spectroscopy, Physical Electronics, 1995, and references therein] The observed Si2p, Si2s and O1s peaks are consistent with the presence of silica, whereas the N1s peak originates from the nitrogen in the co-initiater.[5] The presence of small amounts of Na and Cl may result from the synthesis of the mesoporous silica material.

One has to take into account that XPS is very surface sensitive and thus the measured values refer to the outer part of the approximately 200 nm thick film. Nevertheless, a substantial amount of co-initiator is located in the bottom part of the mesoporous film which is indirectly seen by cyclic voltammetry after polymerization as discussed below as well as by ellipsometry.

Influence of irradiation energy on polymerization inside and outside of mesopores

Variation in irradiation density between 2.9 to 8.6 mW/cm² using 4',5'-dibromfluoresceine and DMAEMA for polymerization resulted in a comparable polymer amount under the applied experimental conditions. The irradiation time was adjusted from 6 minutes and 44 seconds up to 20 minutes, and the same total irradiation energy (57.6 mW/cm²) was guaranteed. Within the applied experimental conditions no clear influence of irradiation energy was observed.

Infrared spectroscopy

The silica matrix shows inorganic framework bands corresponding to transverse optical Si−O−Si modes observed in the 800 cm^{-1} (v_s) and in the 950−1300 cm^{-1} zone (v_{as}).Inorganic silica bands in the 800 cm^{-1} (v_s) and in the 950−1300 cm^{-1} zone (v_{as}), accompanied by a longitudinal optical mode, which appears as a shoulder at 1250 cm^{-1} and Si−O−H bands at 950 cm^{-1} are observed for all samples showing the presence of the silica matrix.[6-7] The bending O−H bands, corresponding to adsorbed water, are centered at 1660 cm^{-1}. Stretching v_{CH} bands (2900−3000 cm^{-1}), corresponding to methylene residues belong to polymer present after visible light induced polymerization.

Polymer Effect on Ionic Permselectivity

Ionic permselectivity and its manipulation is one relevant parameter for applications into "Lab-on-Chip" devices. Successful polymerization should be reflected in polymer-dominated mesopore permselectivity for small charged molecules. This tuning of ionic permselectivity by polymer type and –amount[8] offers the potential of gradual and local permselectivity adjustment in case of locally controlled polymerization in mesoporous silica. In dependence of solution pH, mesoporous silica pore walls are either neutral (pH < 3) or negatively charged due to deprotonated silanol groups. This leads to electrostatically closed mesopores for solution pH values larger than four and negatively charged molecules in solution as extensively described in the literature and shown in the supporting information (Figure S1).[9-10] On the other hand oppositely charged small molecules are pre-concentrated inside the mesopores. This behavior can be explained by the combination of structure and chemical functions and thus pore sizes in the range of the Debye screening length. In case of acidic pH and neutral pores, small molecules independent of their charge can diffuse into the mesopores. Changing surface functionalization thus leads to modifications in mesopore accessibility. Figure 5 depicts representative results on mesopore accessibility obtained by cyclic voltammetry with cationic $[Ru(NH_3)_6]^{2+/3+}$ and anionic $[Fe(CN)_6]^{4-/3-}$ probe molecules

detected at the working electrode (ITO) which is located as substrate-support below the mesoporous film.

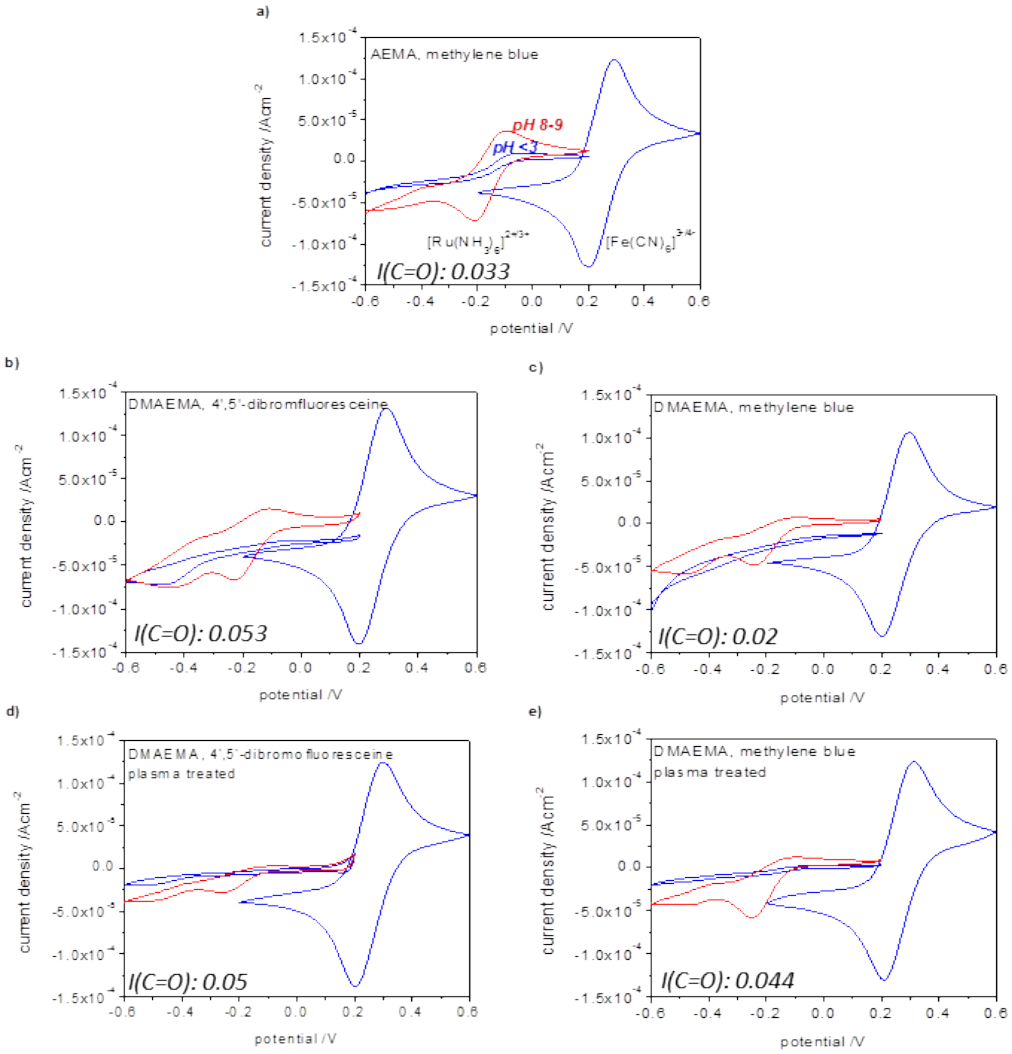

Figure S2: Cyclic voltammetry measurements at a scanrate of 25 mV/s and a pH < 3 (blue) and pH 8-9 (red) for AEMA initiated with methylene blue (a) and DMAEMA initiated with methylene blue (b, d) and 4',5'-dibromfluoresceine (c,e) without (b, c) and with (d, e) plasma treatment to prevent polymer functionalization at the external mesoporous silica film surface.

Polymer modification of a mesoporous silica film resulted in mesopore accessibility determined by the polymer charge. PAEMA with a pKa around 7.5 is expected to result in positively charged polymer at a measured pH of 3 and a neutral polymer at an adjusted pH of 8-9. Additionally, the polymer amount should have an influence, especially on the amount of adsorped, negatively charged probe molecule. Intuitively, an increasing adsorption with increasing polymer amount would be expected. Taking confinement effects on charge density and pKa into account this experimental observation might deviate from this simple expectation. Looking at the measured cyclic voltammograms for AEMA initiated with

methylene blue an exclusion of positively charged $[Ru(NH_3)_6]^{2+/3+}$ at pH of ~3 and thus for positively charged AEMA is observed as expected. At pH 8-9 a diffusion into the mesoporous film for this probe molecule due to a neutral polymer according to its pKa is observed matching the expectation (Figure 5a). In case of the negatively charged probe molecule $[Fe(CN)_6]^{3-/4-}$ a signal enhancement as compared to unmodified silica or the pure ITO electrode at acidic conditions is observed due to electrostatic pre-concentration. In case of a basic pH of 8-9 the negatively charged $[Fe(CN)_6]^{3-/4-}$ molecules are able to diffuse towards the ITO electrode and an Ip in the range of unmodified ITO or neutral unmodified silica film is observed indicating a neutral pore.

In comparison to AEMA, DMAEMA shows a slightly higher pKa of 8.2. Nevertheless, at an acidic pH of 3 PDMAEMA should be positively charged like AEMA and at a basic pH of 9 the polymer should be neutral. Figure 5b-e displays the measured cyclic voltammograms which show an exclusion of positively charged probe molecule $[Ru(NH_3)_6]^{2+/3+}$ at pH 3 and detection of current at a basic pH of 9 although the exact maximum current varies slightly for different samples. For the negatively charged probe molecule $[Fe(CN)_6]^{3-/4-}$ a pre-concentration at acidic pH of 3 is observed, visible in the detected maximum current which is higher as compared to an unmodified mesoporous silica film or an unmodified ITO electrode. This pre-concentration is slightly higher for larger polymer amounts as detected by slightly higher maximum currents with increasing C=O absorption at 1725 cm^{-1} relative to the silica absorption at 1060 cm^{-1} as detected by infrared spectroscopy (Figure 4). Thereby, 4',5'-dibromfluoresceine-initiation resulted in slightly larger polymer amount under the applied experimental conditions as compared to initiation by methylene blue and thus polymer modified mesoporous films with fluoresceine initiation showed slightly higher preconcentration as compared to DMAEMA modified samples after initiation with methylene blue (Figure 5b,c and 5d,e). Plasma treatment and thus destruction of the co-initiator at the external mesoporous film surface does not seem to have a determining effect on the observed electrostatic mesopore accessibility gating for the generated polymer amounts as visible by comparing Figure 5 b, d and Figure 5 c,e. This clearly supports the infrared spectroscopy and ellipsometry results showing clearly polymer functionalization inside the mesoporous film which is a requirement for surface plasmon-induced local surface-polymer functionalization.

EXPERIMENTAL DETAILS

Chemicals. Tetraethoxysilane (TEOS) and Pluronic® F127 were purchased from Alfa Aesar and Sigma Aldrich, respectively. Methylene blue was purchased from Sigma Aldrich, 2-chlorothioxanthone from abcr, and 4',5'-dibromfluoresceine from Alfa Aesar. The co-initiator 3-[Bis(2-hydroxyethyl)amino]propyl-triethoxysilane was purchased from abcr. The monomers 2-Aminoethylmethacrylat (AEMA), 2-(Dimethylamino)ethylmethacrylat (DMAEMA) and [2-(Methacryloyloxy)ethyl]-trimethylammonium chloride (METAC) were purchased from Sigma Aldrich.

Mesoporous silica films were synthesized via a sol gel chemistry based on the oxide precursor tetraethoxysilane (TEOS) in the presence of the template Pluronic® F127. The precursor solutions (1 TEOS: 0.0075 F127: 24 EtOH: 5.2 H_2O: 0.28 HCl) were stirred for 24 h and used to produce films by evaporation induced self-assembly (EISA)[11] on ITO, glass, silicon wafer, or gold-SiOx-coated LaSFN9 substrates at 40-50% relative humidity and 298 K (2 mm/s withdrawing speed). Freshly deposited films were stored at 50% relative humidity in a chamber for 1 h. Then a stabilizing thermal treatment was carried out in two successive 1 h steps at 60 and 130 °C. Consecutively, the temperature was increased to 350 °C with a gradient of 1 °C/min. The films were finally stabilized at 350 °C for 2 h. Subsequently, the films were rinsed with ethanol and stored under ambient conditions. With these conditions the resulted film thickness was around 200 nm and the porosity ~50% as measured by ellipsometry.[3] The surface area was determined by Krypton BET adsorption to be 36 m² per 1 m² substrate surface which corresponds to ~440 m²/g.

Surface modification with [bis(2-hydroxyethyl)amino]propyl-triethoxysilane as co-initiator was performed by immersing the mesoporous silica films for approximately one hour into a 0.01 wt% solution of bis-(2-hydroxyethyl)-3-aminopropyltriethoxysilane in dry THF at 80°C. Afterwards the films were rinsed with THF and extensively extracted in ethanol.

Polymerization by visible light. Initiator solutions are prepared by dissolving 0.0003 g dye (methylene blue or 4',5'-dibromoflureseceine) in 50 ml aqueous 0.1 M $NaHCO_3$ solution. For initiation with 2-chlorothioxanthone 0.0003 g are dissolved in 50 mL of a 1:1 mixture of acetonitrile and an aqueous 0.1 M $NaHCO_3$-solution. The monomer is as well dissolved in an aqueous $NaHCO_3$ solution. Monomer concentrations of 200 g/L (METAC) and 250 g/L (AEMA and DMAEMA) were used. Before polymerization the dye solution and the monomer solution are mixed in a ratio of 1:9 and the solution is degassed for 1h by nitrogen bubbling under the exclusion of light and in the presence of the co-initiator functionalized mesoporous film. For polymerization the mesoporous film is irradiated with visible light (Lumatec Lamp S 400) for ten minutes. The mesoporous film is located in a distance of 10 cm, positioned perpendicular to the waveguide. After polymerization the mesoporous film is extensively extracted in water.

Surface Plasmon Resonance Spectroscopy (SPR) induced polymerizations were performed in the Kretschmann configuration.[12] For these measurements the sample glass slide (LaSFN9 glass, Hellma Optik GmbH Jena, refractive index n = 1.8449, corresponding to ε = 3.4037) was installed into a homemade flow cell (volume ~ 40 µl) and the backside was optically (refractive index) matched with the base of the glass prism (refractive index n = 1.8449, corresponding to ε = 3.4037). Monochromatic and linear, transverse-magnetic polarized (Glan-Thompson polarizer, B. Halle) laser light (He/Ne laser, JDSU, 1125P, λ = 632.8 nm) was directed through the prism onto the sample substrate. By variation of the angle of incidence θ (two-cycle goniometer, resolution 0.005°, Huber) and detecting the intensity of the reflected laser light I(θ) with a photodiode (BPW 34B silicon photodiode, Siemens) an angular dependent spectrum was recorded in air and after adding the polymerization solution containing methylene blue as initiating dye. The polymerization solution was flown constantly during one experiment at a flow rate of 1-8 µL/min. Polymerization was performed at the surface plasmon resonance angle for 2 h and an incident angle of 73°, with laser beam energy of up to 4 mW. SPR measurements were performed at 145 µW, corresponding to 100% reflectivity. After polymerization for 2 h polymer was already visible by eye and the sample was extracted in water and characterized by DRIFT and AFM.

X-ray photoelectron spectra (XPS) were recorded using a Surface Science Laboratories SSX-100 X-ray photoelectron spectrometer equipped with a monochromatic Al Kα X-ray source (100 W). The X-ray spot size was 250−1000 µm. The binding energy scale of the system was calibrated using Au $4f_{7/2}$ = 84.0 eV and Cu $2p_{3/2}$ = 932.67 eV from foil samples. Charging of the powder samples was accounted for by setting the peak of the C 1s signal to 285.0 eV. A Shirley background was subtracted from all spectra. Peak fitting was performed with Casa XPS using 70/30 Gauss−Lorentz product functions. Atomic ratios were determined from the integral intensities of the signals, which were corrected by empirically derived sensitivity factors.

UV-VIS spectroscopy was performed using a Varian Cary 50 SCAN UV−VIS spectrometer. The UV−vis spectra were recorded in a range of 300 to 800 nm. All measurements were performed at 22 °C and the solution concentration was identical to the polymerization solution described above.

Diffuse reflectance infrared Fourier transform spectroscopy measurements (DRIFTS) were performed on a Nicolet Magna 560 instrument, equipped with a liquid nitrogen cooled MCT-Adetector. DRIFTS measurements were performed by depositing scratched film samples on a KBr filled DRIFTS sample holder.

Cyclic voltammetry was performed using a potentiostate TQ_03 with an Ag/AgCl reference electrode. All probe solutions were prepared with a concentration of 2 mM in 100 mM KCl as

supporting electrolyte resulting in a pH 5-6 solution. Acidic or basic conditions (pH 3 and pH 8) were adjusted by adding a drop of a concentrated HCl or NaOH solution directly before starting the measurement. Quantitative variations in permselectivity were studied by following the changes of voltammetric peak currents associated to cationic $[Ru(NH_3)_6]^{2+/3+}$ and anionic $[Fe(CN)_6]^{4-/3-}$ redox probes, diffusing across the mesoporous film.[13]

Gel permeation chromatography (GPC) was performed with DMF/LiCl (3 g/L) as the mobile phase (flow rate 0.5 mL min-1) on a GRAM 1000 A VS with a GRAM 1000 A HS column (PSS) and a 1200 Agilent RID detector column set from PSS at 30 °C. Calibration was carried out using PMMA standards (from Polymer Standard Service, Mainz).

ESI mass spectroscopy was measured after degrafting of mesoporous film bound polymers using a Finnigan LCQ Deca.

References

[1] R. R. Patil, S. Turgman-Cohen, J. Srogl, D. Kiserow, J. Genzer, *Langmuir* **2015**, *31*, 2372-2381.
[2] J. E. Spanier, I. P. Herman, *Phys. Rev. B* **2000**, *61*, 10437.
[3] C. Boissiere, D. Grosso, S. Lepoutre, L. Nicole, A. B. Bruneau, C. Sanchez, *Langmuir* **2005**, *21*, 12362-12371.
[4] A. Brunsen, A. Calvo, F. J. Williams, G. J. A. A. Soler-Illia, O. Azzaroni, *Langmuir* **2011**, *27*, 4328-4333.
[5] C. Hess, U. Wild, R. Schlögl, *Micropor. Mesopor. Mater.* **2006**, *95*, 339-349.
[6] A. Calvo, P. C. Anglomé, V. M. Sánchez, D. A. Scherlis, F. J. Williams, G. J. A. A. Soler-Illia, *Chem. Mater.* **2008**, *20*, 4661-4468.
[7] P. Innocenzi, *J. Non-Cryst. Solids* **2003**, *316*, 309-319.
[8] A. Andrieu-Brunsen, S. Micoureau, M. Tagliazucchi, I. Szleifer, O. Azzaroni, G. J. A. A. Soler-Illia, *Chem. Mater.* **2015**, *27*, 808-821.
[9] M. Etienne, A. Quach, D. Grosso, L. Nicole, C. Sanchez, A. Walcarius, *Chem. Mater.* **2007**, *19*, 844-856.
[10] J. Elbert, F. Krohm, C. Rüttiger, S. Kienle, H. Didzoleit, B. N. Balzer, T. Hugel, B. Stühn, M. Gallei, A. Brunsen, *Adv. Funct. Mater.* **2014**, *24*, 1591-1601.
[11] C. J. Brinker, Y. Lu, A. Sellinger, H. Fan, *Adv. Mater.* **1999**, *11*, 579-585.
[12] W. Knoll, *Annu. Rev. Phys. Chem* **1998**, *49*, 569-638.
[13] D. Fattakhova-Rohlfing, M. Wark, J. Rathousky, *Chem. Mater.* **2007**, *19*, 1640-1647.